FE Upper Bound Limit Analysis for Automated Identification of Collapse Mechanisms in Masonry Structures

Martina Buzzetti(✉), Natalia Pingaro, and Gabriele Milani

Department of Architecture, Built Environment and Construction Engineering, Politecnico di Milano, Milan 20133, Italy
martina.buzzetti@polimi.it

Abstract. A finite element method based on upper bound limit analysis is proposed to estimate the collapse acceleration that induces local failure mechanisms in existing masonry structures. The structural assessment follows the Italian building code, with the added flexibility of not relying on predefined failure mechanisms. The structural model is composed of infinitely rigid hexahedron elements interconnected by quadrilateral interfaces, where plastic deformations are concentrated according to a to a failure criterion such as the Mohr-Coulomb model. The limit analysis problem is formulated following the kinematic approach and solved through a well-established linear programming algorithm. This approach allows the automatic detection of the collapse acceleration and the corresponding failure mechanism, depending on the tensile strength. Through an iterative extrapolation procedure, the solution for the no-tension material model is obtained – as required by Italian standards and commonly assumed for masonry structures in the technical literature. The methodology can also account for the presence of tie-rods. Furthermore, an innovative filtering algorithm is introduced to consider only the elements implicated in the failure mechanism, allowing for the evaluation of the collapse spectral acceleration. The methodology is used for the seismic assessment of a portion belonging to complex historical building in Italy.

Keywords: Limit analysis · Masonry constructions · Local failure mechanisms · Seismic assessment

1 Introduction

In many European and Mediterranean countries, much of the built heritage consists of masonry structures and is located in regions with moderate to high seismic hazard [1]. Historic masonry structures often exhibit weak connections between walls, floors, and roofs, as they were originally conceived to support only vertical loads. As a result, when subjected to seismic forces, these structures fail to develop a box-like behavior and instead experience local collapse mechanisms [2]. In some cases, even when connections are adequate, out-of-plane failures may still occur due to the high slenderness of the walls [3].

© The Author(s), under exclusive license to Springer Nature Switzerland AG 2026
O. Gervasi et al. (Eds.): ICCSA 2025 Workshops, LNCS 15886, pp. 354–367, 2026.
https://doi.org/10.1007/978-3-031-97576-9_24

To ensure the preservation and structural safety of these buildings, it is crucial to determine the accelerations that trigger such failure mechanisms and to develop suitable strengthening strategies. Several analytical and numerical approaches are available for this purpose, including Finite Element Modeling (FEM), Discrete Element Modeling (DEM), and kinematic limit analysis. In addition, recent analytical formulations based on Airy stress functions have been proposed to evaluate the seismic capacity of purely compressed structures [4].

FEM is widely used as it enables the assessment of both global structural behavior and local failure mechanisms [5–7]. However, defining appropriate constitutive models for masonry nonlinear behavior within FEM involves numerous parameters. Among the most commonly used for masonry structures is the Concrete Damage Plasticity (CDP) model, as it can accurately replicate their mechanical behavior when properly calibrated [8, 9]. Nevertheless, this model does not strictly allow for a no-tension material assumption. A low value of tensile strength must be assigned to ensure numerical convergence, which can sometimes lead to an overestimation of the collapse acceleration for out-of-plane failure modes.

DEM, on the other hand, is highly effective in modeling masonry structures since it directly represents the interaction between individual masonry units [10–12]. Despite its accuracy, DEM-based approaches are often computationally expensive and require access to costly commercial software, which can be a limiting factor.

Due to these challenges, the Italian building code requires the safety assessment of out-of-plane local collapses through at least a kinematic linear analysis based on predefined failure mechanisms [13, 14]. While this method is computationally efficient and straightforward, it may either overestimate or underestimate the critical acceleration required to trigger local failures articularly in structures with complex geometries where the affected portion of the structure is not easily identifiable in advance.

The structural safety of complex historical masonry constructions under seismic actions is assessed in this paper with a numerical approach based on the combination of limit analysis with finite elements [15–17], which have proven effective also in evaluating the effectiveness of tie-rod strengthening interventions [18]. The primary objective is to verify out-of-plane local failure mechanisms in accordance with Italian standards while overcoming the previously discussed limitations. The approach proposed follows the upper bound limit analysis approach and has been implemented in MATLAB, following the methodology proposed in [19, 20]. It allows the estimation of the collapse load assuming a no-tension material as required by Italian regulations through a linear extrapolation, accounting also for the presence of eventual tie-rods, as well as the estimation of the failure mechanism and the collapse spectral acceleration one again in agreement with the Italian building code through a filtering algorithm to avoid the overestimation of the structural bearing capacity, proposed for the first time in [21].

The present methodology offers a computationally efficient alternative to DEM while requiring only the definition of the structural geometry and the Mohr-Coulomb failure criterion, thereby overcoming the challenges associated with FEM constitutive models. Additionally, it eliminates the need for predefined failure mechanisms, making it a more flexible and effective tool for assessing seismic vulnerability in historic masonry structures.

2 Upper Bound Limit Analysis-Based Methodology Description

This study presents a numerical methodology that integrates the limit analysis upper bound theorem with finite elements to evaluate the seismic capacity of existing masonry structures. The most frequent failure modes for such types of construction are out-of-plane failures. The approach is consistent with Italian standards [13, 14] and offers the advantage of not requiring predefined failure mechanisms. As described in [19], a classical limit analysis problem can be formulated for any masonry structure if (i) the structure is discretized into hexahedral elements, which are considered infinitely resistant, as depicted in Fig. 1, and (ii) inelastic deformations are lumped only at element interfaces.

The active failure mechanism and collapse load are provided by the limit analysis problem, which can be tackled using either static or kinematic theorem. Given the adopted assumptions, plasticity is lumped into a discrete number of interfaces, ensuring that the kinematic and static solutions converge. As a result, the kinematic approach is preferred in this study for its ease of application, while the static formulation could be derived through a self-dual linear programming problem.

The problem sees six unknowns per hexahedral element, which are the velocities of the centroid along the reference axes (U_x^i, U_y^i, U_z^i) and the rotational rates about the centroid (ϕ_x^i, ϕ_y^i, ϕ_z^i), as illustrated in Fig. 1. External forces are assumed to be solely vertical forces $f_0^{(i)}$, representing self-weight, and horizontal volume forces $f_\Gamma^{(i)}$, dependent on the load multiplier Γ mimicking seismic actions. In agreement with Italian standards [13, 14], two horizontal load distributions can be modelled for $f_\Gamma^{(i)}$. The first, referred to as G1, represents the primary force distribution, which is mass proportional and is directly proportional to the height, forming an inverse triangular pattern. The second, denoted as G2, corresponds to a secondary force distribution, which remains constant along the height while still being mass proportional.

Constraining the velocity jump at element interfaces ensures plastic compatibility, as plastic dissipation is permitted only in these regions. The compatibility conditions are applied to a faceted approximation of the quadrilateral interface, represented by four triangular facets sharing a common vertex at the centroid. Internal actions, velocity jumps, and power dissipation are evaluated in four collocation points, positioned at the corners of the quadrilateral interface. Internal actions are given by the product of the triangle area with the corresponding normal and tangential stresses. These calculations are made referring to an appropriate local reference frame, denoted as $\boldsymbol{n} - \boldsymbol{q} - \boldsymbol{r}$, as shown in Fig. 1.

The jump of velocity at the collocation point C_{P_K} belonging to two adjacent elements (i) and (j), if the versor $\boldsymbol{n}$ is outward from element (i), is computed as:

$$\Delta U_{CPK} = R^{(j)}u^{(j)} - R^{(i)}u^{(i)} \tag{1}$$

where the velocity at the collocation point C_{P_K} for element (i) is evaluated as:

$$U^{(i)}_{CPK} = \begin{bmatrix} n^T \\ q^T \\ r^T \end{bmatrix} \begin{bmatrix} 1\,0\,0 & 0 & z_{P1} - z_{G_{Ei}} & -(y_{P1} - y_{G_{Ei}}) \\ 0\,1\,0 & -(z_{P1} - z_{G_{Ei}}) & 0 & x_{P1} - x_{G_{Ei}} \\ 0\,0\,1 & y_{P1} - y_{G_{Ei}} & -(x_{P1} - x_{G_{Ei}}) & 0 \end{bmatrix} \begin{bmatrix} U^{(i)} \\ \phi^{(i)} \end{bmatrix} = R^{(i)} u^{(i)} \tag{2}$$

With $U^{(i)} = \begin{bmatrix} U^i_x\ U^i_y\ U^i_z \end{bmatrix}^T$, $\phi^{(i)} = \begin{bmatrix} \phi^i_x\ \phi^i_y\ \phi^i_z \end{bmatrix}^T$, as well as the coordinates of the collocation point C_{P_K} are identified as x_{Pk}, y_{Pk}, z_{Pk} while $x_{G_{Ei}}, y_{G_{Ei}}, z_{G_{Ei}}$ are the coordinates of the centroid of the element.

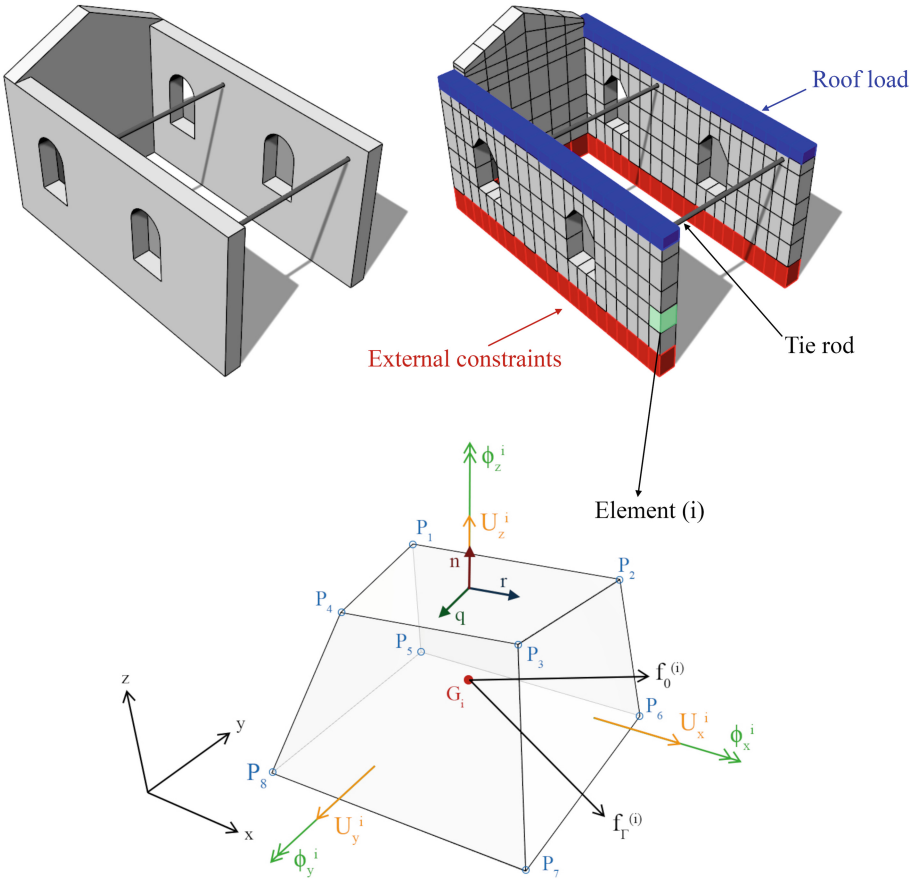


Fig. 1. Structure discretization in hexahedron elements featuring six kinematic variables.

The proposed method enables the consideration of various construction materials for the elements and properties at the interfaces, as visually represented by various colors in Fig. 1. At the interfaces between adjacent elements, a failure criterion such as the Mohr-Coulomb model, with cut-offs in tension and compression, is assumed. It is defined by

tensile f_t and compressive f_c strengths, friction angle Φ, and cohesion c. It is supposed in the present approach that cohesion equals the tensile strength. For a detailed insight into this assumption, the reader is referred to [21]. The plastically admissible strength domain can be defined by a set of linear inequalities in the local reference frame $\boldsymbol{n}-\boldsymbol{q}-\boldsymbol{r}$:

$$\boldsymbol{A}_{in}^{I}\begin{bmatrix} N_I \\ Q_I \\ R_I \end{bmatrix} \leq \boldsymbol{b}_{in}^{I} \tag{3}$$

In Eq. 3, $N_I = A_I\sigma_I, Q_I = A_I\tau_{qI}, R_I = A\tau_{rI}$ are the internal actions, whereas $\sigma_I, \tau_{qI}, \tau_{rI}$ are the stresses acting along $\boldsymbol{n}, \boldsymbol{q}$ and $\boldsymbol{r}$, respectively, and A_I is the area of the quadrilateral interface.

The plastic multipliers $\dot{\lambda}_I$ are linked to the velocity jumps between adjacent elements (i) and (j) due to the associate flow rule assumed:

$$\boldsymbol{R}^{(j)}\boldsymbol{u}^{(j)} - \boldsymbol{R}^{(i)}\boldsymbol{u}^{(i)} - \boldsymbol{A}_{in}^{I\,T}\dot{\lambda}_I = 0 \tag{4}$$

Moreover, plastic multipliers are non-negative at each interface:

$$\dot{\lambda}_I \geq 0 \forall I = 1, \ldots, N_{in} \tag{5}$$

Therefore, the power dissipated by internal actions at the interfaces is given by:

$$P_{in} = \sum_{I=1}^{N_{in}} P_{in}^{I} = \sum_{I=1}^{N_{in}}\sum_{k=1}^{4} \frac{A_I}{4}\boldsymbol{b}_{in}^{I\,T}\dot{\lambda}_{Ik} \tag{6}$$

While the power associated with external volume forces is calculated as:

$$P_0 = \sum_{i=1}^{N_e} V_i \boldsymbol{f}_0^{(i)T}\boldsymbol{U}^{(i)} \tag{7}$$

$$P_\Gamma = \Gamma\sum_{i=1}^{N_e} V_i \boldsymbol{f}_\Gamma^{(i)T}\boldsymbol{U}^{(i)} \tag{8}$$

The normalization condition allows for the selection of the collapse mechanism from the infinite set of homothetic failure modes. It is assumed that the power expended by the loads dependent on the load multiplier is unitary when $\Gamma = 1$.

From the internal and external powers balance, the load multiplier Γ is estimated. By maximizing the power balance according to the kinematic theorem, the collapse load multiplier is found.

External boundary conditions are translated as velocity constraints for those elements externally constrained:

$$\mathrm{A}_{\mathrm{bc}}^{(\mathrm{h})}\mathrm{U}^{(\mathrm{h})} = 0 \tag{9}$$

In Eq. 9, the apex (h) identifies the constrained element while the dimension of the matrix $A_{bc}^{(h)}$ changes according to the constraint type.

The present method considers the tie-rods as rigid truss elements. This is translated into velocity constraints on the elements (k) and (l) connected by the ties:

$$\mathrm{A}_{\mathrm{tr}}^{(\mathrm{k})}\mathrm{U}^{(\mathrm{k})} - \mathrm{A}_{\mathrm{tr}}^{(\mathrm{l})}\mathrm{U}^{(\mathrm{l})} = 0 \tag{10}$$

Finally, the classic limit analysis formulated as follows is solved through a linear programming algorithm in the software Matlab.

$$\min\left\{\Gamma = \sum_{I=1}^{N_{in}}\sum_{k=1}^{4}\frac{A_I}{4}\boldsymbol{b}_{in}^{I\,T}\dot{\lambda}_{Ik} - \sum_{i=1}^{N_e} V_i \boldsymbol{f}_0^{(i)T}\boldsymbol{U}^{(i)}\right\} \tag{11}$$

$$\text{s.t.}\begin{cases} \mathrm{R}^{(\mathrm{j})}\mathrm{u}^{(\mathrm{j})} - \mathrm{R}^{(\mathrm{i})}\mathrm{u}^{(\mathrm{i})} - \mathrm{A}_{\mathrm{in}}^{\mathrm{I}\,\mathrm{T}}\dot{\lambda}_{\mathrm{I}} = 0 \forall I = 1, \ldots, \mathrm{N_{in}} \\ \sum_{\mathrm{i}=1}^{\mathrm{N_e}} \mathrm{V_i}\mathrm{f}_{\mathrm{l}}^{(\mathrm{i})\,\mathrm{T}}\mathrm{U}^{(\mathrm{i})} = 1 \\ \mathrm{A}_{\mathrm{bc}}^{(\mathrm{h})}\mathrm{U}^{(\mathrm{h})} = 0 \forall \mathrm{h} \in \mathrm{b.c.} \\ \mathrm{A}_{\mathrm{tr}}^{(\mathrm{k})}\mathrm{U}^{(\mathrm{k})} - \mathrm{A}_{\mathrm{tr}}^{(\mathrm{l})}\mathrm{U}^{(\mathrm{l})} = 0 \forall \mathrm{k,l} \in \text{tie rods} \\ \dot{\lambda}_{\mathrm{I}} \geqslant 0 \, \forall I = 1, \ldots, \mathrm{N_{in}} \end{cases} \tag{12}$$

2.1 Results Extrapolation for NTM (No-Tension Materials)

Regarding the masonry strength domain, it is important to highlight that assuming zero tensile strength, namely a no-tension material, is a well-established hypothesis in classical literature. Moreover, Italian regulations require the assessment of the acceleration that activates local collapses considering masonry with vanishing tensile strength. However, enforcing null tensile strength can lead to spurious sliding between adjacent elements or cause numerical convergence issues.

To address this, the iterative procedure based on limit analysis, originally introduced by [20] for determining failure loads under no-tension material conditions, is implemented. This approach relies on two key assumptions: (i) only minimal sliding between adjacent elements is permitted, and (ii) the estimation of the collapse load for a material with null tensile strength is based on a failure mechanism that is not significantly influenced by spurious sliding due to an excessively low tensile strength.

According to [21], the load multiplier Γ is linear in f_t and in any mechanical parameter that quantitatively defines the homothetic contraction or expansion of the strength domain. Performing limit analysis iteratively while gradually decreasing f_t enables the generation of $\Gamma - f_t$ plots while simultaneously identifying the corresponding failure mechanisms. The $\Gamma - f_t$ relationship remains linear within all ranges of f_t where the same failure mechanism remains active.

2.2 Spectral Acleration Estimation

Performing a standard safety assessment from limit analysis, essential for practical design, requires careful consideration, especially for local failure mechanisms. These mechanisms often occur in buildings with weak floor stiffness and poor wall interlocking,

involving significantly less mass than global failure scenarios. Additionally, upper-floor mechanisms may experience amplification effects. Overestimating structural capacity by considering the entire mass is a common issue, which occurs together with the selection of pre-determined collapse mechanisms suggested by Italian standards. To address this, a filtering procedure is necessary to accurately capture complex, unforeseen failure mechanisms by isolating critical structural portions.

According to Italian standards [13, 14], the acceleration triggering the local failure mechanism is equal to the spectral acceleration a_0^*:

$$a_0^* = \frac{\alpha_0 \cdot g}{e^* \cdot FC} \tag{13}$$

In Eq. 13, α_0 represents the load multiplier at collapse, g is the acceleration of gravity, FC is the confidence factor, defined according to [13, 14], and e^* is the effective mass ratio.

$$e^* = \frac{g \cdot M^*}{\sum_{i=1}^{n+m} P_i} \tag{14}$$

In Eq. 14, $n + m$ defines the total number of self-weights P_i that contribute to horizontal forces acting on the elements of the kinematic chain because of the seismic action, while M^* is the participating mass.

$$M^* = \frac{\left(\sum_{i=1}^{n+m} P_i \delta_{x,i}\right)^2}{g \cdot \sum_{i=1}^{n+m} P_i \delta_{x,i}^2} \tag{15}$$

In Eq. 15, $\delta_{x,i}$ is the horizontal virtual velocity of the point where the i-th weight P_i is applied. To avoid the overestimation of a_0^*, only the elements of the structure featuring a velocity $\delta_{x,i}$ greater than a predefined limit (20% of the maximum one, as found in [21]) are considered for evaluating the participating mass M^*.

Furthermore, the real distribution of horizontal forces acting on the construction is properly considered by substituting the collapse load α_0 in Eq. 13 with the quantity $a_g/g = \frac{baseshear}{verticalload}$. Indeed, for the evaluation of local mechanisms, Italian standards assume only a G2 horizontal load distribution, resulting in a drawback for the method presented here.

Finally, a local mechanism is not triggered if:

$$a_0^* \geq \frac{a_g S}{q} \tag{16}$$

In Eq. 16, a_g denotes the maximum ground acceleration at the bedrock at the location site, S is a coefficient accounting for the soil type and topography class, while q denotes the behavior factor (fixed at 2 according to [14]).

To assess the reliability and accuracy of the proposed method, it has been benchmarked against experimental results available in the literature from the dynamic testing of a simple U-shaped wall on a shaking table. A detailed description of the proposed numerical procedure, as well as the comparison with the experimental results, are provided in [21].

3 Case Study: Implementation of the Approach

The methodology described in the previous section is applied to a real case study, named the old monastery of Santa Maria della Pace, Piacenza (Italy). The monastery was constructed in the 16th century. Significant structural changes were not made on the portion of the structure that still stands nowadays [5, 22]. The old monastery features a cloister layout developed on two levels, as illustrated in Fig. 2. The cloisters and the corridors on the first floor feature a vaulted ceiling with cross vaults, while pavilion vaults constitute the covering of most of the rooms, only a few of them have timber floors. The pitched timber roof varies in height, adapting to the building elevation geometry. The portion of the structure analyzed is highlighted in green in Fig. 2. It is one of the most vulnerable parts. Indeed, it features a basilica layout architecture with one of the longitudinal walls supported by a cloister vault covering a big room on the ground floor, as shown in Fig. 2.

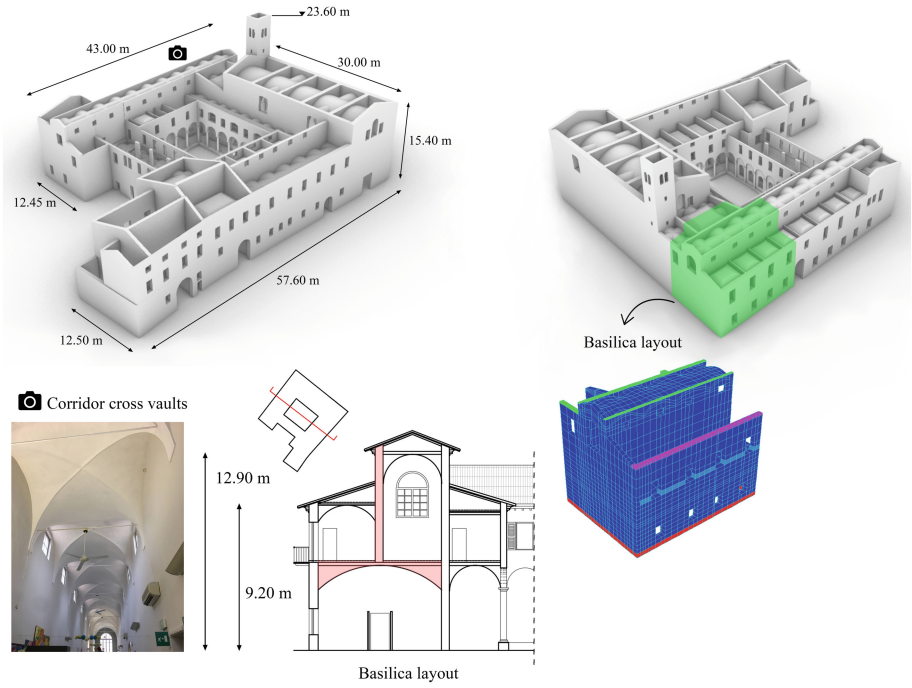


Fig. 2. Santa Maria della Pace Monastery: overview and numerical model of the analyzed portion.

The local failure mechanisms triggered by the spectral acceleration a_0^* are studied under two horizontal load distributions (G1 and G2) acting perpendicular to the longitudinal walls of the basilica layout. The structural performance of this portion of the monastery is verified against the seismic design acceleration prescribed by the regulation for the site of Piacenza for the life safety (SLV) limit state. The design acceleration is characterized by a 475-year return period T_R and a bedrock PGA a_g equal to 0.092 g. According to Italian regulations and the site stratigraphy, the soil type is classified as

C while the topography class is T1. Consequently, the coefficient S is equal to 1.5. Therefore, in agreement with Eq. 16, the failure mechanism is not activated if:

$$a_0^* \geq \frac{a_g S}{q} = 0.677\, m/s^2 \tag{17}$$

The collapse accelerations a_g/g at progressively decreased tensile strength are depicted in Fig. 3. The analyses are performed under horizontal forces with G1 and G2 distributions orthogonal to the longitudinal walls, exhibiting the highest vulnerability under out-of-plane loading. The collapse acceleration a_g/g for a no-tension material ($f_t = 0MPa$) is estimated by means of a linear extrapolation of the results. During the linear extrapolation process, collapse accelerations linked to collapse mechanisms influenced by spurious sliding of the elements are excluded.

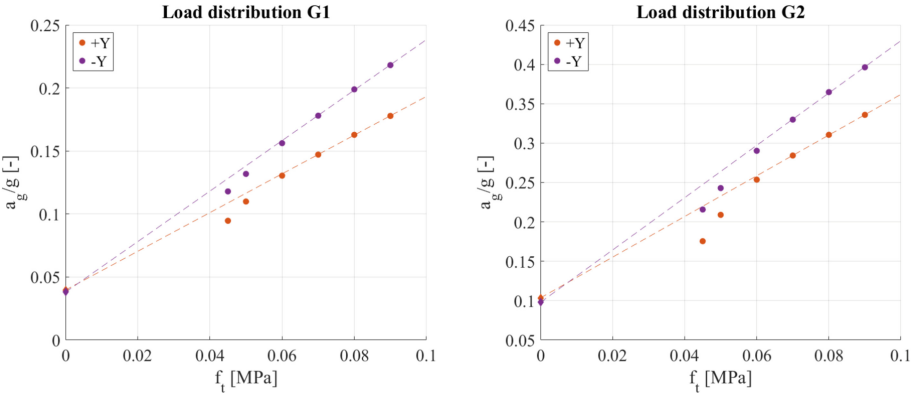


Fig. 3. Seismic assessment of the Basilica Layout: collapse acceleration vs tensile strength.

The spectral acceleration that activates the local collapse mechanism is evaluated based on the collapse acceleration a_g/g, estimated for a material with zero tensile strength, and is compared with the design value defined in Eq. 17. Figure 4 presents the estimated spectral accelerations and the active local collapse mechanisms of the structure under the G1 and G2 horizontal load distributions, for both the positive and negative Y directions. The G2 load distribution leads to a collapse spectral acceleration greater than the design value, indicating that the structure is verified. In contrast, for the G1 load distribution, the structure is not verified against the design seismic acceleration, as the spectral acceleration is lower.

Since the construction is not verified for the G1 load distribution, the contribution of existing tie-rods to the structural load-bearing capacity is assessed. The disposition of tie rods is shown in Fig. 5. Three tie rods are placed on the ground floor in correspondence with the cloister vault, and four ties are placed in the corridor on the first floor under the cross vaults. The collapse accelerations a_g/g for reduced values of tensile strength are shown in Fig. 6, together with the results for the same structure without tie-rods.

The collapse mechanism and the collapse spectral acceleration of the strengthened structure, computed assuming zero tensile strength, are depicted in Fig. 7. The chains

give a significant improvement of the structural load-bearing capacity when the load acts in the Y-positive direction (about 44%). Indeed, a different collapse mechanism is triggered with respect to the structure without tie-rods (see Fig. 4). Instead, the increment is negligible (about 11%) when the structure is loaded in Y negative direction. The failure mechanism is quite the same for both the reinforced and unreinforced structure. However, for both loading directions, the structure is not verified, and the design acceleration is greater than the collapse spectral acceleration.

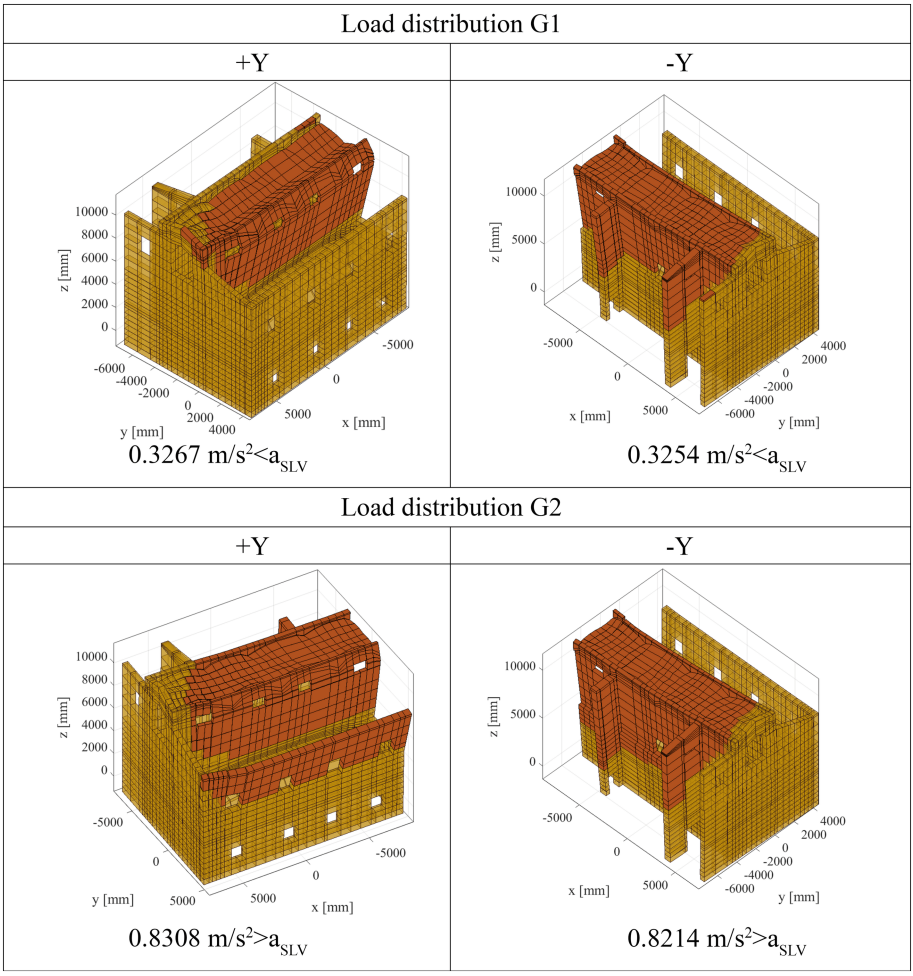


Fig. 4. Seismic assessment of the Basilica Layout: failure mechanisms and spectral accelerations.

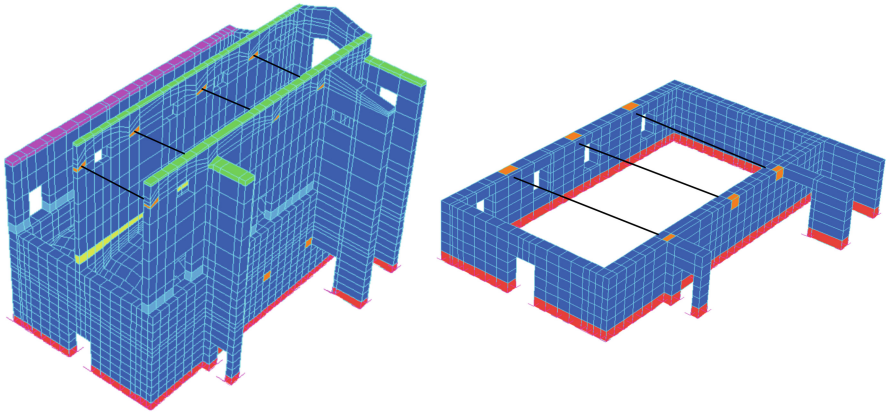


Fig. 5. Disposition of the tie-rods.

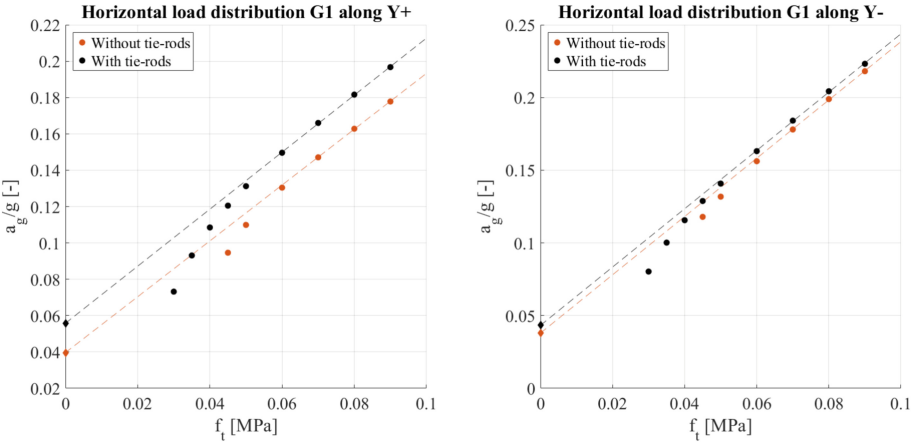


Fig. 6. Seismic assessment of the Basilica Layout with tie-rods: collapse load vs the tensile strength.

4 Conclusions

This study introduces an upper-bound finite element limit analysis approach, incorporating a velocity filtering routine to evaluate the seismic safety of masonry structures with complex geometries, while also accounting for the presence of eventual chains. The method aligns with Italian standards while eliminating the need for predefined failure mechanisms. The structure is discretized into infinitely resistant hexahedral elements, with plasticity lumped to their interfaces, making the upper and lower bounds of the limit analysis problem coincide.

Solving the classic limit analysis problem formulated following the kinematic theorem through a linear programming problem, the collapse acceleration and failure mechanisms are found. Internal actions are computed from the static dual linear programming problem.

Since Italian standards prescribe negligible tensile strength without sliding, the collapse acceleration is indirectly determined through linear extrapolation, preventing premature algorithm failure and spurious sliding. The MATLAB-based implementation requires only the mesh definition and Mohr-Coulomb strength parameters, facilitating rapid analysis. Additionally, an automated filtering strategy identifies elements significantly contributing to the collapse mechanism, ensuring an accurate evaluation of the collapse acceleration for ultimate limit state verifications.

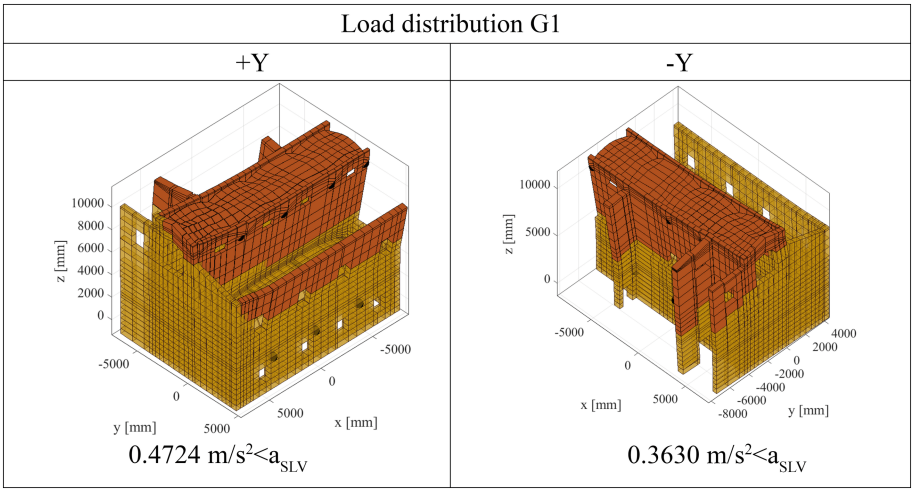


Fig. 7. Basilica Layout with tie-rods seismic assessment: failure mechanisms and collapse spectral accelerations under G1 horizontal load distribution.

The methodology is applied to a real case study in Piacenza, Italy, namely the former Monastery of Santa Maria della Pace. The structure features a complex geometry, making standard analysis methods unreliable. The most critical portion of the structure is studied, which is characterized by a basilica layout. The results highlight the necessity of strengthening interventions, as local collapses could be triggered by the design seismic action specified in the Italian building code, even if the existing tie-rods are accounted for.

Acknowledgments. The study was partially developed within the research activities carried out in the frame of 2024–2026 ReLUIS Project – WP10 masonry structures (Coordinator – Prof. Guido Magenes), specifically by means of the research carried out in WP10.1.1 and WP10.2 Masonry Structures (Task Coordinators – respectively Prof. Serena Cattari and Prof. Sergio Lagomarsino).

The Italian Department of Civil Protection has funded such a project.

Finally, the study was partially developed with the financial support of the Italian Ministry of Scientific Research MUR within the research project PRIN-2022 (https://www.dabc.polimi.it/en/progetto/advanced-mechanical-models-and-computational-methods-for-large-scale-3d-printing-of-innovative-concrete-structures/) titled "Advanced mechanical models and computational methods for large-scale 3D printing of innovative con crete structures (COM^3D-CREATE)" (National PI: Prof. Andrea Chiozzi, Local PI: Prof. Gabriele Milani). Finanziato dall'Unione europea Next Generation EU, Missione 4 Componente 1 CUP D53D23004070006.

Disclosure of Interests. The authors have no competing interests to declare that are relevant to the content of this article.

References

1. Shabani, A., Kioumarsi, M., Zucconi, M.: State of the art of simplified analytical methods for seismic vulnerability assessment of unreinforced masonry buildings. Eng. Struct. **239**, 112280 (2021)
2. Acito, M., Buzzetti, M., Chesi, C., Magrinelli, E., Milani, G.: Failures and damages of historical masonry structures induced by 2012 northern and 2016–17 central Italy seismic sequences: critical issues and new perspectives towards seismic prevention. Eng. Fail. Anal. **149**, 107257 (2023)
3. Sorrentino, L., D'Ayala, D., de Felice, G., Griffith, M.C., Lagomarsino, S., Magenes, G.: Review of out-of-plane seismic assessment techniques applied to existing masonry buildings. Int. J. Architectural Heritage **11**, 2–21 (2017)
4. Olivieri, C., Cocking, S., Fabbrocino, F., Iannuzzo, A., Placidi, L., Adriaenssens, S.: Seismic capacity of purely compressed shells based on airy stress function. Continuum Mech. Thermodyn. **37**, 21 (2025)
5. Acito, M., Buzzetti, M., Cundari, G.A., Milani, G.: General methodological approach for the seismic assessment of masonry aggregates. Structures **57**, 105177 (2023)
6. Clementi, F., Gazzani, V., Poiani, M., Lenci, S.: Assessment of seismic behaviour of heritage masonry buildings using numerical modelling. J. Build. Eng. **8**, 29–47 (2016)
7. Milani, G., Valente, M.: Comparative pushover and limit analyses on seven masonry churches damaged by the 2012 Emilia-Romagna (Italy) seismic events: possibilities of non-linear finite elements compared with pre-assigned failure mechanisms. Eng. Fail. Anal. **47**, 129–161 (2015)
8. Acito, M., Bocciarelli, M., Chesi, C., Milani, G.: Collapse of the clock tower in Finale Emilia after the Emilia Romagna earthquake sequence: numerical insight. Eng. Struct. **72**, 70–91 (2014)
9. Castellazzi, G., D'Altri, A.M., de Miranda, S., Chiozzi, A., Tralli, A.: Numerical insights on the seismic behavior of a nonisolated historical masonry tower. Bull. Earthq. Eng. **16**, 933–961 (2018)
10. Schiavoni, M., Giordano, E., Roscini, F., Clementi, F.: Advanced numerical insights for an effective seismic assessment of historical masonry aggregates. Eng. Struct. **285**, 115997 (2023)
11. Azevedo, J., Sincraian, G., Lemos, J.V.: Seismic behavior of blocky masonry structures. Earthq. Spectra **16**, 337–365 (2000)
12. Oktiovan, Y.P., Messali, F., Pulatsu, B., Lemos, J.V., Rots, J.G.: A contact-based constitutive model for the numerical analysis of masonry structures using the distinct element method. Comput. Struct. **303**, 107499 (2024)

13. Ministero delle Infrastrutture e dei Trasporti: Decreto 17 gennaio 2018 Aggiornamento delle "Norme tecniche per le costruzioni". Gazzetta Ufficiale Della Repubblica Italiana (2018)
14. Ministero delle Infrastrutture e dei Trasporti: Circolare 21 gennaio 2019 n.7: Istruzioni per l'applicazione dell'Aggiornamento delle "Norme Tecniche per le Costruzioni" di cui al decreto ministeriale 17 gennaio 2018. Gazzetta Ufficiale Della Repubblica Italiana (2019)
15. Chiozzi, A., Grillanda, N., Milani, G., Tralli, A.: UB-ALMANAC: an adaptive limit analysis NURBS-based program for the automatic assessment of partial failure mechanisms in masonry churches. Eng. Fail. Anal. **85**, 201–220 (2018)
16. Lo Monaco, A., et al.: Seismic assessment of Romanian Orthodox masonry churches in the Banat area through a multi-level analysis framework. Eng. Fail. Anal. **153**, 107539 (2023)
17. Aita, D., Bruggi, M., Garavaglia, E.: Collapse analysis of masonry arches and domes considering finite friction and uncertainties in compressive strength. Eng. Fail. Anal. **163**, 108462 (2024)
18. Fabbrocino, F., Olivieri, C., Luciano, R., Vaiano, G., Maddaloni, G., Iannuzzo, A.: Seismic performance of historic masonry buildings: a comparative analysis of equivalent frame and block-based methods. Alex. Eng. J. **109**, 359–375 (2024)
19. Wang, P., Milani, G.: Specialized 3D Distinct element limit analysis approach for a fast seismic vulnerability evaluation of massive masonry structures: Application on traditional pagodas. Eng. Struct. **282**, 115792 (2023)
20. Wang, P., Milani, G.: Seismic vulnerability prediction of masonry aggregates: iterative finite element upper bound limit analysis approximating no tensile resistance. Eng. Struct. **293**, 116595 (2023)
21. Buzzetti, M., Pingaro, N., Milani, G.: Automatic detection of local collapse mechanisms in historical masonry buildings: fast and robust FE upper bound limit analysis. Eng. Fail. Anal. **170**, 109310 (2025)
22. Pingaro, N., Buzzetti, M., Milani, G.: Advanced FE nonlinear numerical modeling to predict historical masonry vaults failure: assessment of risk collapse for a long span cloister vault heavily loaded at the crown by means of a general-purpose numerical protocol. Eng. Fail. Anal. **167**, 109070 (2025)